THE DEVELOPMENT OF CENTRAL PEAKS IN LUNAR CRATERS

J. W. BOND

School of Mathematical and Physical Sciences, University of Sussex, Brighton, U.K.

(Received 21 May, 1981)

Abstract. From a consideration of equations describing the supersonic impact of a solid body on to a solid target, the difference between final crater depth and distance vertically below the original impact at which the rarefaction wave front, resulting from the reflection of the backward propagating shock wave in the meteorite, first intersects the forward travelling shock wave front in the target has been determined. A correlation between this difference and the height of central peak features in the majority of fresh lunar craters has been established. On the basis of this, it is proposed that the intersection of these two wave fronts locally inhibits the ejection of material from behind the shock front during the excavation phase of crater formation, leading to the appearance of a centrally located peak of uplifted material. Subsequent post-impact development of the interior morphological features has been shown to be consistent with the size-scale of development of complex crater features on the lunar and other planetary surfaces. By considering only craters which exhibit this correlation, a scaling between peak height and impact energy has been derived.

1. Introduction

Since the early 1960's when the Lunar Orbiter satellites provided us with a vast amount of photographic data of the cratered surface of the Moon, varied and conflicting theories have been put forward attempting to explain the lunar crater morphology (see, for example, Guest *et al.*, 1980). One particular aspect of the morphology that has stimulated much discussion has been the nature and origin of the central peaks that are observed to rise up from the floor in many of the craters.

Of the various schools of thought relating to the formation of these peaks that have developed over the years, only those which argued crater formation by hypervelocity impact are still maintained today. Of the various hypotheses (Pike, 1977, 1980), two of the most favoured at the present time are that the peaks were formed by wall collapse of the transient cavity (Quaide *et al.*, 1965; Grieve *et al.*, 1977; Melosh, 1977; McKinnon, 1978) or in response to the rapid shock compression and decompression (rarefaction) experienced by the material early on in the crater forming event (Milton *et al.*, 1972; Ullrich *et al.*, 1977). Post impact events such as isostatic decompression (Baldwin, 1971) are today though to play little or no part in the formation of the peaks (Pike, 1980).

Central peak craters have now been observed on most planets and satellites in the solar system where detailed investigations of the surface have been carried out. Images from Mariner and Viking missions have revealed central peak craters on other planets and satellites in the inner solar system (Hartmann, 1977), whilst more recently, Voyager images have revealed these structures on the Galilean satellites of Jupiter (Smith *et al.*, 1979) and the satellites of Saturn (Sutton, 1980).

In the present paper we examine the shock wave mechanics of central peak formation

The Moon and the Planets **25** (1981) 465–476. 0165–0807/81/0254–0465$01.80.
Copyright © 1981 by D.. Reidel Publishing Co., Dordrecht, Holland, and Boston, U.S.A.

from a consideration of equations derived by Andriankin (1978) for the supersonic impact of a solid projectile on to a solid target. The results from this are then compared with central peak structures in lunar craters and a possible explanation for the height of the peaks in terms of the intersection of compression and rarefaction wave fronts is proposed. Finally, the possibility of using this approach to analyse the height of central peaks in craters on other satellites and planets is discussed.

2. Equations Describing Supersonic Impact and Crater Formation

In a recent publication, Andriankin (1978) investigated the physics of a solid body impacting on to a solid target surface. Despite the obvious limitations and difficulties in accurately determining the equation of state of the surface during impact, Andriankin developed the following equations (in the c.g.s. system of units) which describe the dimensions of craters formed by the normal impact of a compact meteorite* on to a solid target at supersonic velocities. That is to say, when the mass speed behind the shock wave exceeds the speed of sound in both the meteorite and the target.

Andriankin has shown that the final (post-impact) depth of the resulting crater (d) can be written as

$$d = m^{1/3} v^{2/3} \sigma^{-1/3} A, \tag{1}$$

where m and v are respectively the mass and velocity of the meteorite and σ is a parameter which depends on the strength and thermodynamic characteristics of the target material. A is a constant which takes into account the meteorite shape and density and is given by

$$A^3 = \frac{3[1 + \frac{2}{3}\delta\epsilon^2(z'/r)^3]}{\pi(\gamma + 1)(1 + \epsilon^2)}, \tag{2}$$

where

$$\delta = \frac{r}{h} \tag{3}$$

is taken to be equal to 0.5; ϵ is the target to meteorite density ratio and γ the effective adiabatic exponent of the plasma generated by the impact; z' is the depth vertically below the original position of impact at which the rarefaction wave front resulting from the reflection of the backward propagating shock wave in the meteorite (Gault *et al.*, 1968) first intersects the forward travelling shock wave front in the target and is given by

$$z' = r\left\{\frac{2 + (\gamma + 1)\sqrt{\frac{\gamma - 1}{2\gamma}}}{(\gamma + 1)\delta\epsilon} + \frac{\gamma + 3}{\sqrt[4]{\frac{\gamma + 1}{\gamma - 1}}}\left(1 + \frac{\gamma + 1}{\sqrt{2\gamma(\gamma - 1)}}\right)\right\}. \tag{4}$$

* A compact meteorite, according to Andriankin, is one for which the length (h) is approximately twice the radius (r).

As was stated earlier, these equations are applicable to supersonic impacts which enabled Andriankin to use as an approximation to the equation of state a much simplified expression containing γ.

We now proceed to show that by selecting parameters for these equations that are consistent with the lunar environment, an estimate of the expected height of the central peak in a crater can be obtained.

3. Method of Analysis

Central peak statistics have been taken from the analysis of Wood and Andersson (1978) for 45 class 1 (fresh) lunar craters, this being a revision of data originally presented by Wood (1968) which included class 2 lunar central peak craters. Of the five principle crater types described by Wood and Andersson (1978), only the Triesnecker (TRI) and Tycho (TYC) types (shown in Figure 1) are considered here. All TYC craters possess central peaks (diameter $(D) = 30$ km to > 200 km) and the occurrence of peaks in TRI craters increases from $\sim 50\%$ at $D \sim 10$ km to 100% at $D \sim 30$ km (Wood and Andersson, 1978). The other three principal crater types have been omitted as central peak abundance in them is low varying from zero to $\sim 24\%$.

For a given crater diameter the depth/diameter ratio quoted by Wood and Andersson (1978) was used to determine the crater depth (d).* Substitution of this depth in Equation (1) enabled the impact mass (m) and kinetic energy (E) for various impact velocities to be calculated. Values taken for γ and σ were those quoted by Andriankin (1978) and the target density was assumed to be equal to the meteorite density. From a knowledge of the meteorite mass the value of z' could then be obtained. For crater diameters in the range 15–30 km the appropriate depth/diameter relationship was for TRI craters

$$d = 0.985D^{0.318}, \tag{5}$$

and for the crater diameter range 30–200 km was the TYC crater relationship

$$d = 0.684D^{0.411}. \tag{6}$$

Both of these equations are least squares fits to Class 1 Lunar Craters (Wood and Andersson, 1978).

Figure 2 shows a logarithmic plot of crater diameter versus the difference between the calculated values of d and z' for an impact velocity range of 10–15 km s^{-1}. Superimposed on this is a plot of lunar central peak height versus crater diameter (Wood and Andersson, 1978) and a correlation between the magnitude of $(d - z')$ and height of the peaks can clearly be seen over a crater diameter range of 30–70 km. By increasing the impact velocity spread to 9–20 km s^{-1} (Figure 3) correlation between the two sets of data occurs over an increased diameter range, $\sim$ 20–$\lesssim$ 100 km. This velocity range (9–20 km s^{-1})

* This depth will of course only be good to a first approximation as Equation (1) does not take into account changes in d due to post-impact crater modifications which are present in the final (measured) crater depths.

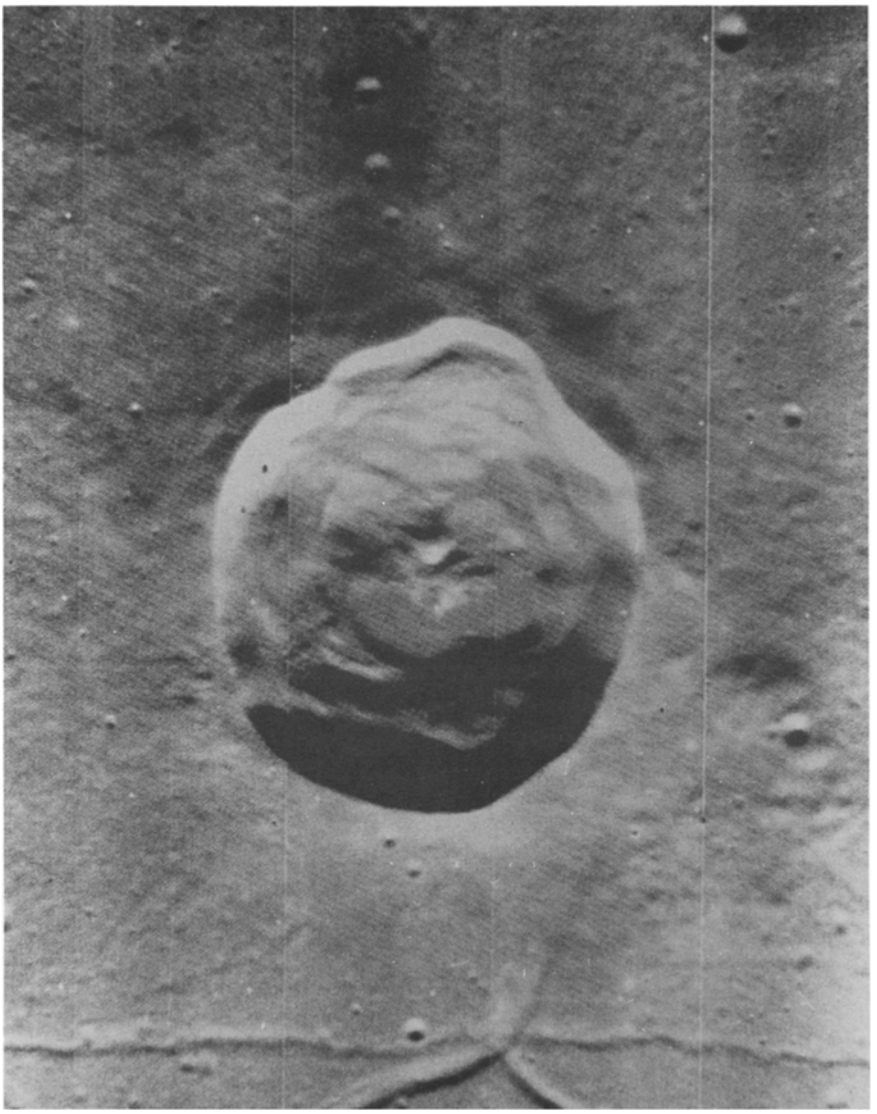

Fig. 1(a) Lunar Crater Triesnecker. A scalloped wall crater ~ 27 km diameter. Typical example of class 1 (fresh) lunar craters with diameters ~ 15 to ~ 50 km. (Lunar Orbiter frame No. IV-102-H1).

lies within the estimated velocity impact limits for meteorites on the lunar surface calculated by Wetherill (1974).

The inference from this correlation is that the eventual height of the central peak is determined by z' and, on the basis of this, a qualitative picture for the possible formation of the peak is now presented.

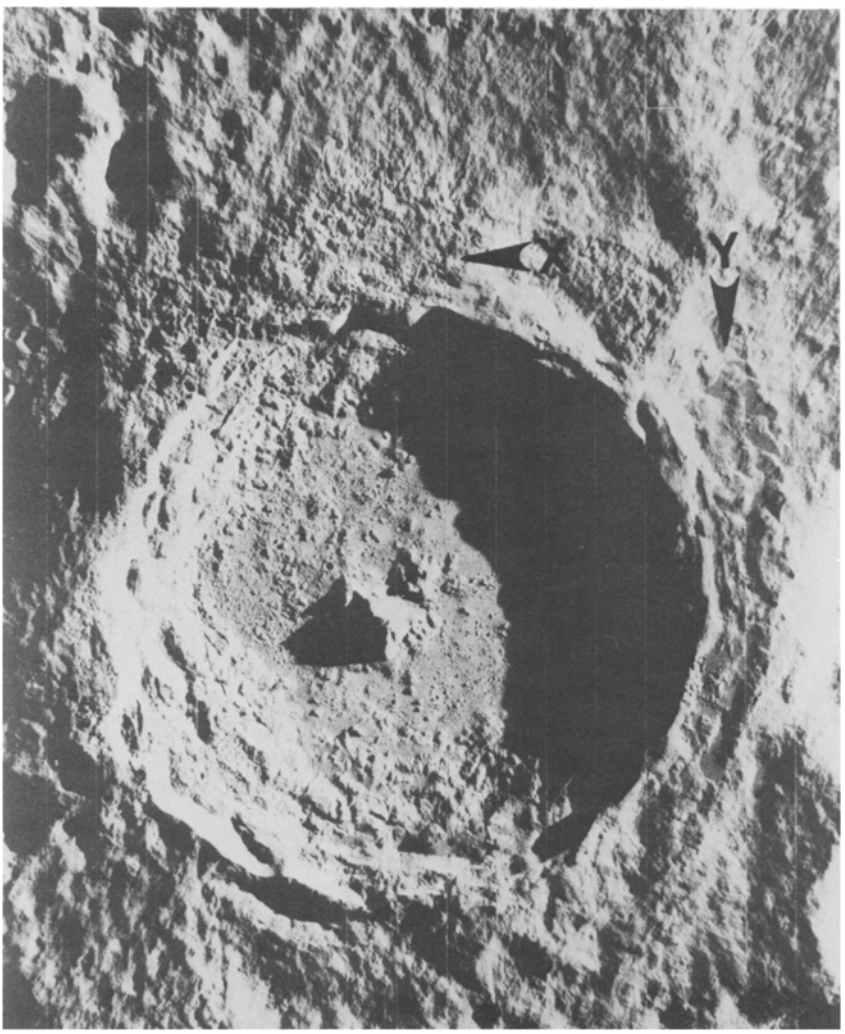

Fig. 1(b) Lunar Crater Tycho. This crater has a complex wall formation of numerous terraces and minor scarps. Diameter ~ 90 km. Typical example of class 1 lunar craters with diameters ~ 30–~ 175 km. Arrow *x* indicates a fracture system along the northern ring and probably caused by the Tycho impact. Arrow *Y* shows a depressed region collaring the inner rim (Lunar Orbiter frame No. V-125-M).

4. Formation of Central Peak

Gault *et al.* (1968) have qualitatively described the formation of an impact crater by dividing the process into three main phases namely: compression, excavation and modification. This same approach has been followed here which, together with calculations based on Andriankin's (1978) equations, forms the basis of an explanation for the development of central peak structures.

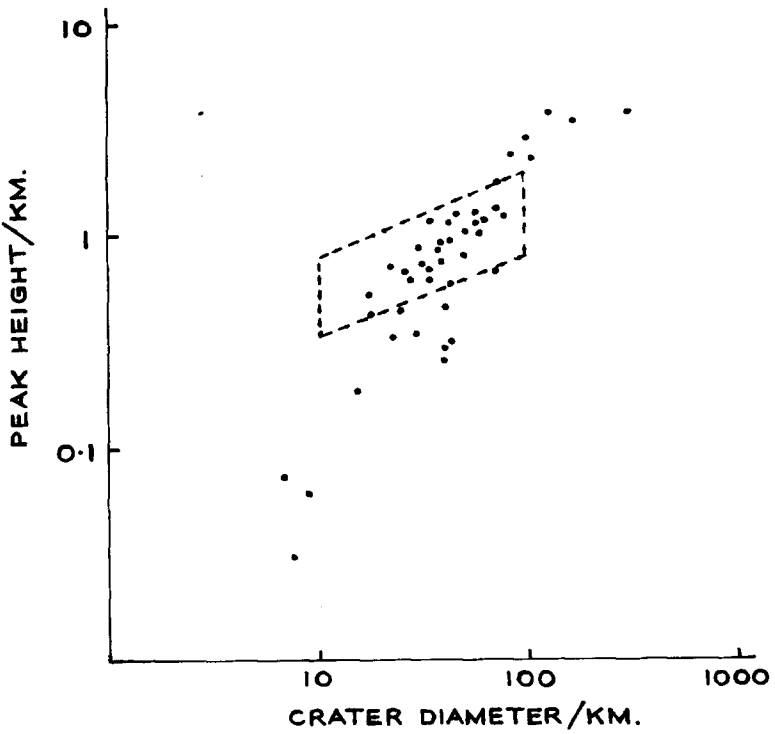

Fig. 2. Logarithmic plot of central peak height compared to crater diameter for 45 class 1 (fresh) lunar craters. Boxed region within dotted lines indicates range of calculated peak heights for impact velocities between 10 and 15 km s^{-1}. Top dotted line corresponds to an impact velocity of 15 km s^{-1}, bottom dotted line corresponds to 10 km s^{-1}.

According to Gault *et al.* (1968), as the meteorite impacts the ground surface, shock waves are produced which transfer the kinetic energy at impact into internal energy of compression with one shock wave travelling down into the target whilst a second moves backwards into the meteorite itself. As these shock waves propagate in their respective directions, discontinuities occur as they make contact with either the free ground surface or the sides of the meteorite which cannot support the state of stress induced by the shock wave. These discontinuities thus give rise to rarefaction or 'stress relief waves' (Andriankin, 1978), which develop behind the shock fronts and are a means of decompressing the shocked material from high to low pressure states. According to Gault *et al.* (1968), once the backward travelling shock front has been reflected from the rear surface of the meteorite, the end of the first (compression) phase of crater formation has been reached and the second (excavation) phase begins to dominate. During this second phase, the pressure behind the expanding shock front in the target material decreases rapidly as a function of distance from the point of impact, which thus results in it's attenuation during this phase.

Reflection of the backward-travelling shock wave at the upper surface of the meteorite

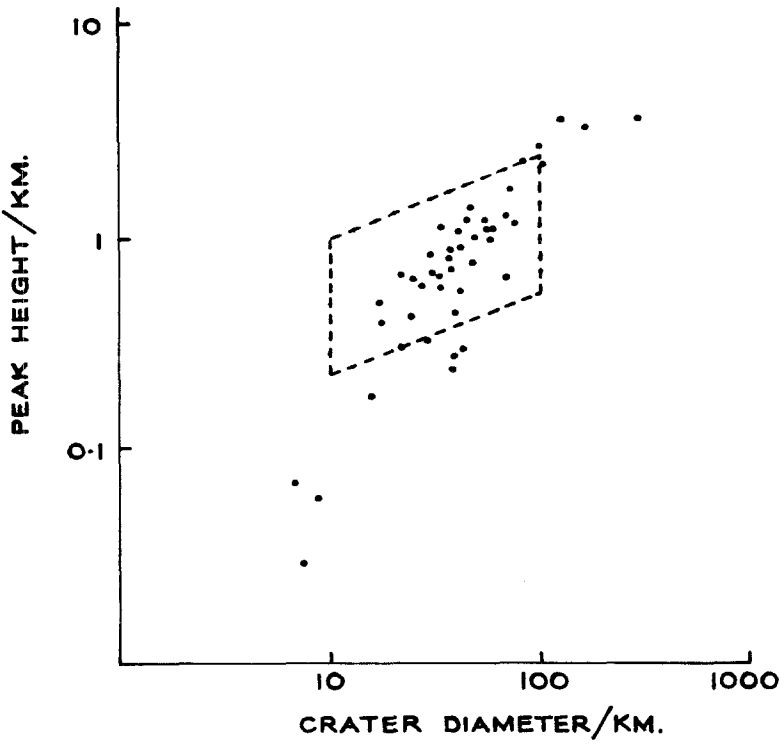

Fig. 3. Logarithmic plot of peak height versus crater diameter. Boxed region indicates range of calculated peak heights for impact velocities between 9 and 20 km s^{-1}. Top dotted line corresponds to an impact velocity of 20 km s^{-1}, bottom dotted line corresponds to 9 km s^{-1}.

causes a forward travelling rarefraction wave to propagate back through the meteorite and then into the target material which, together with other rarefaction waves from the sides of the meteorite and the free ground surface, are collectively responsible for the excavation of the bulk of the shocked material and the formation of the crater (Ahrens and O'Keefe, 1972). The series of rarefaction waves set up throughout the shocked material represent isobars, with the transition from a compressed state behind the shock front to a state of ambient pressure (zero stress) at the free surface being in reality a continuous process. The resulting interaction between this continuum of rarefaction fronts and the shocked sub-surface material causes the latter to convert it's internal energy of compression back to motional kinetic energy and thus to flow from one rarefaction isobar to another in a direction towards the region of ambient pressure (Gault *et al.*, 1968), that is, the ejection of sub-surface material and crater formation.

As the flow of this material follows a direction which is normal to the propagation surface of each of the rarefaction waves it encounters (Gault *et al.*, 1968), immediately below the point of impact (and for a small area surrounding this) the flow of the displaced material will approximate to being in a direction vertically upwards. On the basis

of this and the calculations performed in Section 2, it is suggested that the intersection (at a depth $z = z'$) between the rear stress relief wave (reflected from the meteorite) and the shock front in the target material locally inhibits the ejection of the upward flowing material and corresponds to the position below the original impact at which the central peak begins to form. As the wave fronts expand further into the target the excavation of material from behind the shock front will continue except in a small area of increasing cross section centered on a line vertically below the point of impact and which consists of the peak forming uplifted material. According to Andriankin (1978), for $z > z'$ the attenuation of the shock wave front has a volumetric nature (proportional to $[z'/z]^3$) and leads to an expression (Equation (1)) for the final depth (d) of the crater.

Removal of the impact-induced stresses by the ejection of target material completes the second (excavation) phase of crater formation and introduces the final (modification) phase. According to Gault *et al.* (1968) (see also, more recently, Malin and Dzurisin (1978) and Settle and Head (1979)), the most intense crater modifications take place during this third phase and such effects as central peak formation, floor formation and terracing are the result of the response of the target to the release of the large impact-induced stresses (Head, 1976; Cintala *et al.*, 1977) and gravitational collapse of the crater rim due to the sudden removal of material during the excavation phase (Hartmann, 1972; Gault *et al.*, 1975; Melosh, 1977). However, Pike (1980) has shown that the order of appearance of these complex features on the lunar and other planetary surfaces is not consistent with such an hypothesis. In particular, with increasing crater size, central peaks are observed to appear before terracing (exactly the opposite order to the predictions of the 'collapse hypothesis' (Pike, 1980)), as has been consistently observed on the lunar and Mercurian surfaces (Smith and Sanchez, 1973; Pike, 1975; Wood and Andersson, 1978; Smith and Hartnell, 1978), the Martian surface (Wood and Anderson, 1978; Pike, 1980) and in complex terrestial impact craters (Milton *et al.*, 1972; Roddy, 1979). Thus, in order to be consistent with the measured data, any explanation of the central peaks must be sought in terms of excavation rather than modification phase of crater formation (Pike, 1980).

An additional point made by Pike (1980) is that field studies of complex terrestial impact craters have shown that the material which comprises the central peak can be vertically uplifted by distances of a kilometre or more and also that the peak is the only complex feature to display this uplifting (see Figure 4 of pike, 1980). Such a distribution of material in the central peak is consistent with it's formation during the excavation phase when material, vertically displaced by movement through the stress-relieving decompression wave fronts, is stopped short of actually being ejected because of the interaction between the wave fronts. The region between the top of the peak and the base of the crater thus comprises uplifted material and is in agreement with the findings reported at Gosses Bluff, Australia (Milton *et al.*, 1972); Sierra Madera, Texas, (Howard *et al.*, 1972), and Flynn Creek, Tennessee, (Roddy, 1977, 1979). Subsequent post-impact modifications (third phase) would lead to the development of other complex (possibly gravity induced) morphological features, some of which may arise due to the

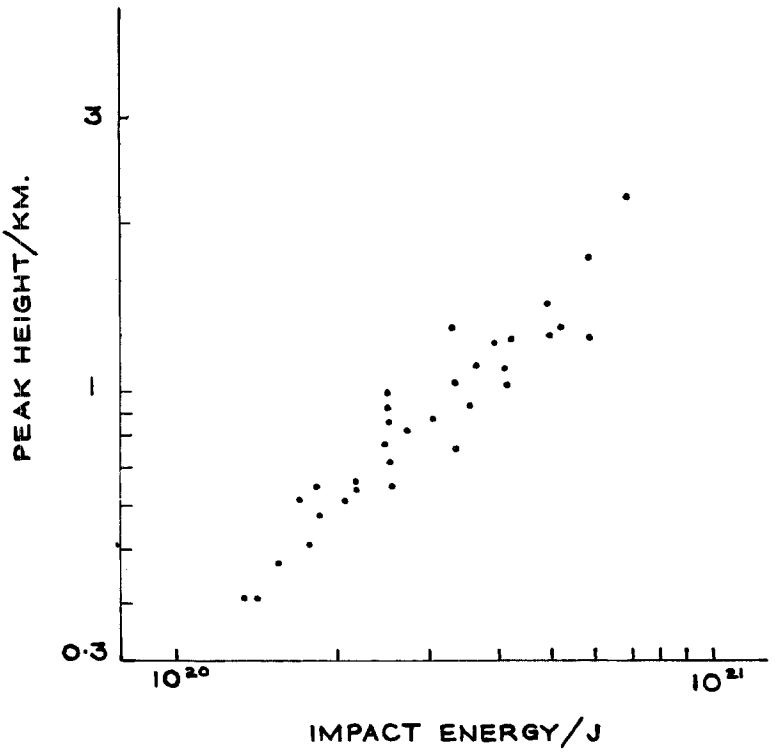

Fig. 4. Logarithmic plot of central peak height versus calculated impact energy for 34 class 1 Lunar central peak craters lying within the boxed region of Figure 3.

formation of the peak itself. For example, the inward movement of the crater sub-floor to compensate for peak uplift could give rise to faulting and hence the appearance of terracing.* More specifically, Wood and Andersson (1978) find that for crater diameters $\gtrsim$ 50 km the dominant mode of crater wall failure changes from scallop formation (TRI craters) to terracing (TYC craters). At the other end of the diameter scale ($D \lesssim 20$ km) Pike (1977) concludes that the slump deposits would almost certainly bury the central peak formation. Such settling to a state of geological stability could well account for the discrepancies between the calculated and observed peak heights, particularly for $D \lesssim 20$ km where the calculated height is typically a few hundred metres greater than the observed height.

5. Peak Height Dependence on Impact Energy

From a knowledge of central peak height and crater diameter for the 34 class 1 craters, lying within the boxed region of Figure 3, it was possible to determine the functionality

* Such a sequence of development for complex morphological features is in agreement with Pike (1980), who notes that while some lunar craters have peaks and no terraces the opposite is an extremely rare occurrence.

between the impact kinetic energy and peak height. This data is presented in Figure 4 as a logarithmic plot of peak height versus impact energy. A least squares fit to the data shows that

$$\text{Peak Ht.} = 3.66 \times 10^{-19}\ E^{0.90}, \tag{7}$$

with a standard error of 0.003 in determining the exponent of the independent variable. The important point to note here is that the scaling between peak height and impact energy is (in this analysis) critically dependent on the scaling between peak height and crater diameter. By considering only those craters which lie within the boxed region of Figure 3, it can clearly be seen that the scaling is significantly different to that obtained by considering all forty-five craters. In other words, the energy scaling equation given above is only valid for craters in which the calculated peak height is a reasonable approximation to the measured value. It is interesting to note that a linear proportionality between peak height and impacting energy has also been suggested by Gault *et al.* (1975) in a discussion of data reported by Wood (1973). However, Gault *et al.*'s analysis was based on the hypothesis that peak height is determined by gravitational potential energy derived from the collapse of the crater walls and, as such, implies that peak formation occurs during the modification phase. Thus, although Gault *et al.*'s (1975) mechanism for peak formation differs from that proposed here, the conclusions regarding the scaling with energy are still in agreement with these calculations.

Calculated values for the mass of the impacting meteorite are of the order of 10^{15} gms. which is in agreement with Hartmann and Hartmann (1968) who state that asteroidal fragments in an intermediate size range ($\sim 10^{15}$ to $\sim 10^{17}$ gms.) provide the meteorites responsible for planetary cratering.

6. Discussion

From a consideration of observed lunar central peak heights and equations describing the supersonic impact of a solid projectile on to a solid target, a correlation between the height of the peak and the vertical depth below the original position of impact at which the shock wave front and reflected rarefaction wave front from the back surface of the meteorite intersect has been established. By considering a possible impact velocity range of between 9 and 20 km s^{-1} close agreement has been obtained for the majority of catalogued class 1 lunar central peak craters (34 out of 45, ~ 77%). On the basis of this correlation, it has been proposed that the intersection of these two wave fronts locally inhibits the ejection of uplifted material during the latter stages of the excavation phase and leads to the formation of a centrally placed region of uplifted material within the newly formed crater. Subsequent changes in the interior morphology of craters during the modification phase would enable other complex features such as terracing or scalloping (Head, 1976; Schultz, 1978) to develop and would therefore be consistent with the measured size scale of development of these features on the lunar and other planetary surfaces (Pike, 1980). The observation on terrestial impact craters that the central peak

is the only complex feature to display significant uplifting further supports this hypothesis with the peak forming first during the mass excavation of material with other complex features developing later during the subsequent modification phase.

Although no explicit dependence of the peak height on gravitational effects has been included in this analysis it is not suggested that peak formation is completely gravity independant, after all, the peak consists of uplifted material and so work against gravity must be performed (Gault *et al.*, 1975; Malin and Dzurisin, 1978). Gravity scaling has been investigated by Hartmann (1972) who proposed that crater diameters scale as $1/g^{1.25}$ with similar morphological features appearing in craters with smaller diameters for planets with larger gravitational accelerations. Similar inverse gravity scaling laws have also been suggested by Carr *et al.* (1977) and Smith and Hartnell (1978). It would be reasonable to suppose, however, that any dependence of the peak height on gravity would be least apparent for lunar craters because of the reduced value of g when compared with other planetary bodies on which central peak craters have been studied in detail (e.g. Mars, Mercury and the Earth). In particular, Andriankin (1978) has shown that the critical crater depth (d^*), below which some portion of the excavated material falls back to the crater floor, scales as the inverse of g and is given by

$$d^* \sim \frac{v^*}{g}, \tag{8}$$

in which v^* is the mass speed at the crater boundary. According to Andriankin (1978), d^* for the lunar environment corresponds to a depth of ~ 1 km and therefore implies that errors in d from ejecta fall-back will only occur for the higher impact energy craters which corresponds to $\sim 50\%$ of those considered here. Bearing in mind these limitations, it is therefore argued that these calculations have to a first approximation provided a basis on which to explain the appearance of central peaks during the excavation phase of crater formation.

Attempting a similar correlation with the central peak data from other planetary surfaces would provide a useful test of this hypothesis. Recent Voyager data from the satellites of Jupiter and Saturn, where the values of g are as low as 0.015 of the value on Earth, could be expected to give at least as good a correlation as has been found here for lunar craters.

Acknowledgements

The author is grateful to Dr P. H. Schultz for permission to reproduce the photographs shown in Figure 1 and to the U.K. Science Research Council for the award of a research studentship.

References

Ahrens, T. J. and O'Keefe, J. D.: 1972, *The Moon* 5, 214.
Andriankin, E. I.: 1978, *Sol. Syst. Res.* 12, 1.

Baldwin, R. B.: 1971, *Phys. Earth Planet. Int.* **4**, 167.
Carr, M. H., Crumpler, L. S., Cutts, J. A., Greeley, R., Guest, J. E., and Masursky, H.: 1977, *J. Geophys. Res.* 82, 4055.
Cintala, M. J., Wood, C. A., and Head, J. W.: 1977, *Proc. Lunar Sci. Conf. 8th.* 3409–3425.
Gault, D. E., Quaide, W. L., and Oberbeck, V. R.: 1968, in B. M. French, N. M. Short (eds.), *Shock Metamorphism of Natural Materials*, Mono Book Corp., Baltimore, pp. 87–99.
Gault, D. E., Guest, J. E., Murray, J. B., Dzurisin, D., and Malin, M. C.: 1975, *J. Geophys. Res.* **80**, 2444.
Grieve, R. A. F., Dence, M. R. and Robertson, P. B.: 1977, in D. J. Roddy, R. O. Pepin, and R. B. Merrill, (eds.), *Impact and Explosion Cratering*, Pergamon, New York, pp. 791–814.
Guest, J. E., Butterworth, P., Murray, J. B., and O'Donnell, W.: 1980, *Planetary Geology*, David and Charles, Newton Abbot.
Hartmann, W. K.: 1972, *Icarus* **17**, 707.
Hartmann, W. K.: 1977, *Scientific American* **236**, 84.
Hartmann, W. K. and Hartmann, A. C.: 1968, *Icarus* 8, 361.
Head, J. W.: 1976, *Proc. 7th Lunar Sci. Conf.*, 2913–2929.
Howard, K. A., Offield, T. W., and Wilshire, H. G.: 1972, *Geol. Soc.. Amer. Bull.* **83**, 2397.
Malin, M. C. and Dzurisin, D.: 1978, *J. Geophys. Res.* **83**, 233.
McKinnon, W. B.: 1978, *Proc. 9th Lunar Planet Sci. Conf.* 3965–3973.
Melosh, H. J.: 1977, in D. J. Roddy, R. O. Pepin, and R. B. Merrill (eds.), *Impact and Explosion Cratering*, Pergamon, New York, pp. 1245–1266.
Milton, D. J., Barlow, B. C., Brett, R., Brown, A. R., Glikson, A. Y., Manwaring, F. A., Moss, F. J., Sedmik, E. C. E., Van Son, J., and Young, G. H., 1972, *Science* **175**, 1199.
Pike, R. J.: 1975, *Mod. Geol.* 5, 169.
Pike, R. J.: 1980, *Icarus* **43**, 1.
Pike, R. J.: 1977, in D. J. Roddy, R. O. Pepin, and R. B. Merrill (eds.), *Impact and Explosion Cratering*, Pergamon, New York, pp. 489–509.
Quaide, W. L., Gault, D. E., and Schmidt, R. A.: 1965, *Ann. N.Y. Acad. Sci.* **123**, 563.
Roddy, D. J.: 1977, in D. J. Roddy, R. O. Pepin, and R. B. Merrill, (eds.), *Impact and Explosion Cratering*, Pergamon, New York, pp. 185–246.
Roddy, D. J.: 1979, *Proc. Lunar Planet. Sci. Conf. 10th.* 2519–2534.
Schultz, P. H.: 1978, *Moon Morphology*, Univ. of Texas Press, Texas.
Settle, M. and Head, J. W.: 1979, *J. Geophys. Res.* **84**, 3081.
Smith, E. I. and Sanchez, A. G.: 1973, *Mod. Geol.* 4, 51.
Smith, E. I.. and Hartnell, J. A.: 1978, *Moon and Planets* **19**, 479.
Smith, B. A., Soderblom, L. A., Johnson, T. V., Ingersoll, A. P., Collins, S. A., Shoemaker, E. M., Hunt, G. E., Masursky, H., Carr, M. H., Davies, M. E., Cook, A. F., 11, Boyce, J., Danielson, G. E., Owen, T., Sagan, C., Beele, R. F., Veverka, J., Strom, R. G., McCauley, J. F., Morrison, D., Briggs, G. A., and Suomi, V. E.: 1979, *Science* **204**, 951.
Sutton, C.: 1980, *New Scientist* 88, 491.
Ullrich, G. W., Roddy, D. J., and Simmons, G.: 1977, in D. J. Roddy, R. O. Pepin, and R. B. Merrill (eds.), *Impact and Explosion Cratering*, Pergamon, New York, pp. 959–982.
Wetherill, G. W.: 1974, *Proc. Soviet-American Conf. on Cosmochemistry of Moon and Planets*, NASA, Washington, pp. 553–571.
Wood, C. A.: 1968, *Commun. L.P.L.* 7, 157.
Wood, C. A.: 1973, *Icarus* **20**, 503.
Wood, C. A. and Andersson, L.: 1978, *Proc. Lunar Planet. Sci. Conf. 9th.* 3669–3709.